THE JOURNAL OF BIOLOGICAL CHEMISTRY
Vol. 276, No. 27, Issue of July 6, pp. 24751–24759, 2001

Printed in U.S.A.

Mechanisms of Cold-induced Platelet Actin Assembly*

Received for publication, December 22, 2000, and in revised form, April 6, 2001
Published, JBC Papers in Press, April 27, 2001, DOI 10.1074/jbc.M011642200

Karin M. Hoffmeister‡, Hervé Falet‡, Alex Toker§, Kurt L. Barkalow‡, Thomas P. Stossel‡, and John H. Hartwig‡¶

From the ‡Division of Hematology, Brigham and Women's Hospital, and the §Department of Pathology, Beth Israel Deaconess Medical Center, Harvard Medical School, Boston, Massachusetts 02115

Various agonists but also chilling cause blood platelets to increase cytosolic calcium, polymerize actin, and change shape. We report that cold increases barbed end nucleation sites in octyl glucoside-permeabilized platelets by 3-fold, enabling analysis of the intermediates of this response. Although chilling does not change polyphosphoinositide (ppI) levels, a ppI-binding peptide completely inhibits cold-induced nucleation. The C terminus of N-WASp, which inhibits the Arp2/3 complex, blocks nucleation by 40%; GDPβS, N17Rac and N17Cdc42 have no effects. Some gelsolin translocates to the detergent-insoluble cytoskeleton after cooling. Chilled platelets from gelsolin-deficient mice have ~50% fewer new actin nuclei compared with platelets from wild-type mice. EGTA completely inhibits gelsolin translocation into the cytoskeleton, and the small amount of gelsolin initially there becomes soluble. Chilling releases adducin from the detergent-resistant cytoskeleton. We conclude that platelet actin filament assembly induced by cooling involves ppI-mediated actin filament barbed end uncapping and *de novo* nucleation independently of surface receptors or downstream signaling intermediates besides calcium. The actin-related changes occur in platelets at temperatures below 37 °C, suggesting that the platelet may be more activable at temperatures at the body surface than at core temperature, thereby favoring superficial hemostasis over internal thrombosis.

As the suspension medium temperature falls below 15 °C platelets abruptly change their shape from smooth discs into spiny spheres with irregular projections and aggregate (1–5). These events resemble platelet responses to thrombin, ADP, collagen, and other stimuli that operate optimally at 37 °C through energy-dependent signaling reactions resulting in actin remodeling. However, cooling slows these reactions and causes most cell types to round up. The response of human blood platelets to chilling has profound medical consequences. It limits the storage of over 90 milion platelet units collected worldwide per year for transfusion to 5 days at room temperature, because longer storage leads to unacceptable amounts of microbial growth. Even 5-day storage of platelets without refrigeration results in occasional septic complications following transfusion (6, 7).

Unactivated discoid platelets have a unique submembrane coil of microtubules. Some microtubules depolymerize at low temperatures, and the microtubule coils of platelets dissolve in the cold (1, 8). At reduced temperatures, cells also become less able to maintain energy-dependent low cytosolic calcium levels, and chilled platelets have increased cytosolic calcium concentrations (4). Since calcium-dependent severing of the actin scaffolding that maintains the discoid shape of the resting platelet is an early step in normal platelet activation, this calcium rise is presumably a mediator of cold-induced platelet activation. In addition to these clues to possible mechanisms underlying cold activation of platelets, recent work has implicated phosphoinositide-mediated actin assembly (9, 10). Platelet stimulation through the PAR-1 receptor activates the Rho GTPase Rac leading to the synthesis of polyphosphoinositides (ppIs).[1] Studies in permeabilized platelets indicated that these lipids induce actin assembly by producing actin nucleation sites equivalent to actin filament fast growing barbed ends. Since these ppIs release barbed end capping proteins such as gelsolin from actin filaments in permeabilized platelets, uncapping of preexisting actin filaments is one pathway proposed from ppIs to actin assembly and is amplifiable by actin filament severing and capping, which increase the number of ends. A second pathway involves ppIs and Cdc42-activated unfolding of Wiskott-Aldrich syndrome protein (WASp) family proteins, which then bind the Arp2/3 complex, resulting in branching barbed end nucleation at the cell cortex that leads to cell movement (11–16). Receptor tyrosine kinases, the Rho family GTPase Cdc42, and probably G-protein-coupled receptors transmit the signals to WASp-Arp2/3 (17–20) and link signaling pathways to cell motility.

Although ppI turnover would predictably diminish in the cold, if degradation declined more than synthesis, net ppI levels might increase, leading to actin assembly. A more plausible explanation is that temperature influences the structure of these lipids. The physical chemistry of lipid presentation affects lipid-protein interactions in general and gelsolin actin binding in particular (21). Tablin *et al.* (22) have proposed evidence for lipid phase changes at the critical temperature for cold-induced platelet activation.

We previously showed that chilled platelets assemble actin from barbed end nuclei (4). In this paper, we document that chilling activates ppI-induced barbed end assembly independently of phospholipid synthesis and GTPase activation. We show that ppIs work through both actin filament barbed end

* This work was supported by National Institutes of Health Grants HL56949 and HL56993 and by the Edwin S. Webster Foundation. The costs of publication of this article were defrayed in part by the payment of page charges. This article must therefore be hereby marked "*advertisement*" in accordance with 18 U.S.C. Section 1734 solely to indicate this fact.

¶ To whom correspondence should be addressed: Division of Hematology, Brigham and Women's Hospital, LMRC 301, 221 Longwood Ave., Boston, MA 02115. Tel.: 617-278-0323; Fax: 617-278-0385; E-mail: hartwig@calvin.bwh.harvard.edu.

[1] The abbreviations used are: ppI, polyphosphoinositide; WASp, Wiskott-Aldrich syndrome protein; OG, *n*-octyl-β-D-glucopyranoside; Pipes, 1,4-piperazinediethanesulfonic acid; GTPγS, guanosine 5′-3-*O*-(thio)triphosphate; GDPβS, guanyl-5′-yl thiophosphate; FITC, fluorescein isothiocyanate; PtdIns-4,5-P_2, phosphatidylinositol 4,5-bisphosphate; HPLC, high pressure liquid chromatography; AM, acetoxymethyl ester; GST, glutathione *S*-transferase; TRAP, thrombin receptor anchoring peptide.

uncapping and Arp2/3-mediated nucleation in chilled platelets. We also provide direct evidence that chilling of platelets activates gelsolin to amplify the actin remodeling response.

EXPERIMENTAL PROCEDURES

Materials—Chemical reagents were purchased from Sigma. Rabbit skeletal muscle actin was isolated and labeled with pyrene as previously described (23). The QRLFQVKGRR 10-mer polyphosphoinositide-binding peptide was synthesized based on residues 160–169 of gelsolin (24). The Arp3 component of the Arp2/3 complex was detected using affinity-purified anti-Arp3 antibody provided by Dr. Matt Welch (University of California, Berkeley, CA). Rabbit polyclonal anti-adducin antibody was kindly provided by Dr. Vann Bennett (Duke University Medical Center, Durham, NC). The monoclonal anti-gelsolin antibody (2C4) was previously described (25).

GST Fusion Proteins—Vectors encoding GST-CA (aa 450–505 of N-WASp) and GST-VCA (aa 392–505 of N-WASp) constructs, derived from the C-terminal end of N-WASp, were kindly provided by Drs. Rajat Rohatgi and Marc Kirschner (Department of Cell Biology, Harvard Medical School, Boston, MA). The GST-RacN17 and -Cdc42N17 expression constructs were kindly provided by Dr. G. Bokoch (Scripps Research Institute, La Jolla, CA). GST proteins were expressed in *Escherichia coli*, purified on glutathione-agarose beads, and stored at −80 °C in concentrations of ≥1 mg/ml. Proteins were thawed at 37 °C and diluted immediately before use. Purity was checked following SDS-polyacrylamide gel electrophoresis through 15% gels and staining with Coomassie Brilliant Blue.

Preparation of Human and Mouse Platelets—Blood was drawn from normal human volunteers by venipuncture into 0.1 volume of Aster-Jandl citrate-based anticoagulant as previously described (26). Platelet-rich plasma was prepared by centrifugation of anticoagulated blood at 100 × *g* for 20 min, and platelets were separated from the plasma proteins by gel filtration (26) through a small Sepharose 2B column. Blood was obtained from wild-type and gelsolin −/− (27) mice by cardiac puncture into 0.1 volume of Aster-Jandl anticoagulant. Mouse platelet-rich plasma was separated from the red blood cells by centrifugation of the blood at 100 × *g* for 6 min, followed by centrifugation of the supernatant and the buffy coat again at 100 × *g* for 6 min. Mouse platelets were isolated from platelet-rich plasma using a metrizamide gradient (28). Briefly, platelets were concentrated between 25 and 10% metrizamide in 140 mM NaCl, 5 mM KCl, 12 mM trisodium citrate, 10 mM glucose, 12.5 mM sucrose, pH 6, by centrifugation at 1,100 × *g* for 12 min. This washing procedure was repeated, and the platelets were resuspended in 140 mM NaCl, 3 mM KCl, 0.5 mM $MgCl_2$, 5 mM $NaHCO_3$, 10 mM glucose, and 10 mM Hepes, pH 7.4. The concentration of human and mouse platelets was adjusted to 3×10^8/ml, and platelets were allowed to rest for 30 min at 37 °C before use.

Permeabilization of Platelets with n-Octyl-β-D-glucopyranoside (OG)—Resting platelets in suspension (90 μl containing 1.5×10^8 platelets) were permeabilized at 37 °C by the addition of one-ninth volume (10 μl) of 2.5% OG in 60 mM Pipes, 25 mM HEPES, 10 mM EGTA, 2 mM $MgCl_2$, 2 μM phallacidin, and protease inhibitors (PHEM buffer) (29). The detergent-platelet suspension was mixed, and the platelets were allowed to extract for 30 s at 37 °C. TRAP, GTPγS, GDPβS, GST-RacN17, GST-Cdc42N17, GST-VCA, or GST-CA were added to the OG-permeabilized cells just before cooling. Permeabilized cells were then cooled for 5 min at ice bath temperatures and rewarmed for 2 min at 37 °C. This procedure resulted in 70–80% of the platelet permeabilized as judged by the incorporation of FITC-phalloidin into the platelets (data not shown).

Phospholipids—Phosphatidylserine (L-α-phosphatidyl-L-serine dipalmitoyl (C16:0)) and PtdIns-4,5-P_2 were obtained from Sigma. Phosphatidylserine and PtdIns-4,5-P_2 were dissolved by sonication in water as described by Janmey and Stossel (21) and were added to the chilled and rewarmed OG permeabilized platelets.

Morphological Studies—25-mm round coverslips were attached to the bottom of 35-mm plastic Petri dishes, each having a 10-mm hole punched in its bottom. The coverslips were coated with 1 mg/ml bovine serum albumin in Dulbecco's phosphate-buffered saline (Life Technologies, Inc.) for 10 min. For experiments using OG, the platelets were permeabilized for 30 s using a final concentration of 0.25% OG. OG suspensions were chilled in plastic tubes for 5 min in an ice bath. In experiments on rewarmed platelets, the tubes were rewarmed to 37 °C for 2 min in a water bath. Platelets were fixed for morphological examination with a final concentration of 3.4% formaldehyde in Dulbecco's phosphate-buffered saline. The fixed platelets were viewed in a Zeiss IM-35 inverted microscope using differential interference contrast optics and a 100× oil immersion objective. Images were captured with a Hamamatsu C2400 CCD camera (Hamamatsu, Japan), processed for background subtraction and frame averaging with a Hamamatsu ARGUS image processor, and digitally stored with a Macintosh computer equipped with a SCION frame grabber LG-3 (SCION, Frederick, MD).

Phospholipid Labeling and Extraction—Human platelets were pelleted and washed from platelet-rich plasma by two sequential centrifugations at 800 × *g* for 10 min in the presence of 1 μM prostaglandin E_1 (Sigma). The purified platelets (~10^9/ml) were incubated for 1 h at 37 °C with 2 mCi/ml of [^{32}P]orthophosphoric acid. ^{32}P in the medium was separated from the platelets by gel filtration over a Sepharose 2B column as described above. The platelets were incubated at ice bath temperatures for 10, 20, 30, or 40 min, and total phospholipids were extracted using two combined washes of chloroform/methanol/HCl. ppIs were deacylated and analyzed by HPLC as described (9, 30, 31).

Measurement of Filament End Numbers—Intact platelets (90 μl containing 1.5×10^8 platelets), incubated at ice bath temperatures for 5 min or treated with 1 unit/ml thrombin for 60 s, were permeabilized with one-ninth volume of 1% Triton X-100 in PHEM buffer. To assess filament end numbers in a temperature-dependent manner, intact platelets (90 μl containing 1.5×10^8 platelets) were incubated for 5 min at 37, 25, 20, 15, 10, 5, or 0 °C with or without the addition of 25 μM TRAP for 60 s and were permeabilized as described above. To assay filament barbed ends, 185 μl of a solution containing 100 mM KCl, 2 mM $MgCl_2$, 0.5 mM ATP, 0.1 mM EGTA, 0.5 mM dithiothreitol, and 10 mM Tris, pH 7.0, was added to 100 μl of the Triton X-100 or OG-lysate. The actin polymerization rate assay was started by the addition of 15 μl of 20 μM monomeric pyrene-labeled rabbit skeletal muscle actin to a final concentration of 1 μM. In this assay, the fluorescence increase is proportional to actin assembled into filaments. Fluorescence was recorded in a LS50 spectrofluorimeter (PerkinElmer Life Sciences) using excitation and emission wavelengths of 366 and 386 nm, respectively. Actin assembly inhibited by 2 μM cytochalasin B is defined as occurring at the barbed end of the actin filament. Activity not inhibited by cytochalasin B is defined as pointed end assembly. The number of free actin filament barbed ends was calculated from the known assembly rates of actin and the cytochalasin sensitivity of this assembly as previously described (23). The barbed and pointed end addition rates used are 10 and 1 monomer s^{-1}, respectively (32).

Immunoblot Analysis of Platelet Cytoskeletal Proteins—Resting and cold-activated platelets (1, 2, 5, and 30 min at ice bath temperatures) or platelets loaded with 40 μM EGTA-AM for 30 min at 37 °C and then chilled (1, 2, 5, and 30 min at ice bath temperatures) were lysed using a final Triton X-100 concentration of 0.1% in PHEM buffer. The lysates were centrifuged at 450,000 × *g* for 30 min at 4 °C, and the resultant pellets and supernatants were separated. The pellet, corresponding to the cytoskeleton, was resuspended to 133% of original volume in 1× SDS-polyacrylamide gel electrophoresis loading buffer (33) containing 5% β-mercaptoethanol. The supernatant was dissolved by the addition of 33% of the original volume of 4× SDS-polyacrylamide gel electrophoresis buffer. The samples were boiled for 5 min. Proteins were displayed by SDS-polyacrylamide gel electrophoresis and transferred onto Immobilon-P membrane (Millipore Corp.). Membranes were blocked using 1% bovine serum albumin in 100 mM NaCl, 20 mM Tris/HCl, pH 7.4, and then probed with specific antibodies and appropriate peroxidase-tagged secondary antibodies. Detection was performed with an enhanced chemiluminescence system (Pierce).

Measurement of F-actin Content—Resting or cold-activated platelets (1, 2, 5, and 30 min at ice bath temperatures) were fixed in 3.4% formaldehyde and permeabilized with 0.1% Triton X-100 in the presence of 10 μM FITC-phalloidin. Bound FITC-phalloidin was quantified by fluorescence-activated cell sorting analysis using a Beckton Dickinson FACSCalibur flow cytometer (Franklin Lakes, NJ). A total of 10,000 events were analyzed for each sample.

RESULTS

Actin Assembly in OG-permeabilized Platelets Induced by Chilling—Fig. 1 shows that most platelets remain discoid at 37 °C after permeabilization with OG (Fig. 1*a*) and that these permeabilized platelets change shape when chilled (Fig. 1*b*). Chilled OG-permeabilized platelets have blebs on their surfaces and elaborate filopodial-like structures that remain after rewarming (Fig. 1*c*). Rewarming is, however, required to detect actin filament barbed ends that nucleate the assembly of pyrene-actin, suggesting that OG-treated platelets reseal upon cooling but become permeable again when rewarmed (Fig. 1*d*).

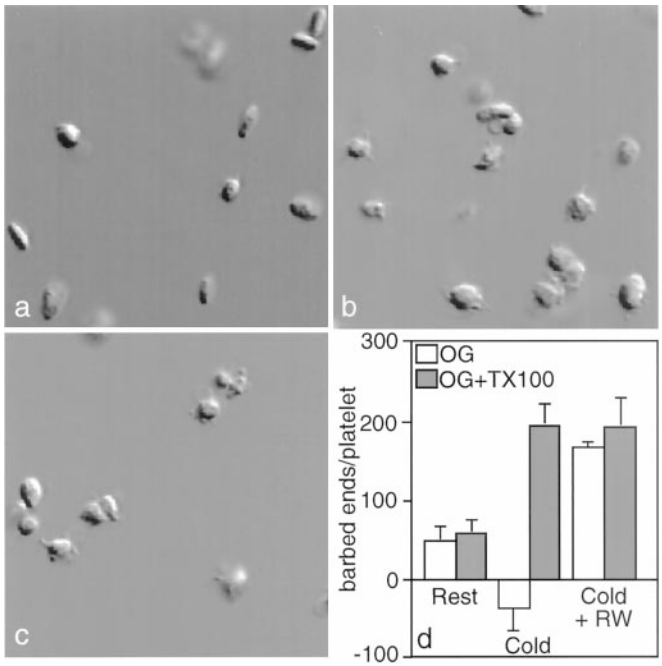

FIG. 1. **Morphology and barbed end actin nucleation capacity of OG-permeabilized platelets before and after chilling.** This gallery of DIC micrographs shows that OG-permeabilized platelets retain their capacity to change shape in the cold by blebbing and forming protrusions at their surfaces and that rewarming does not reverse these changes. *a*, OG-permeabilized platelets remain discoid when maintained at 37 °C. *b*, chilling of OG-permeabilized platelets to ice bath temperatures for 5 min causes the elaboration of membrane protrusions similar to pseudopodia extended by activated cells. *c*, chilled OG-permeabilized cells retain their spiny appearances after rewarming. *d*, chilling of OG-permeabilized platelets causes the exposure of barbed end-directed actin nucleation sites. Shown are barbed end actin filament nucleation site counts in OG-permeabilized platelets maintained at 37 °C platelets (*Rest*), chilled for 5 min in an ice-bath (*Cold*), or chilled for 5 min and then rewarmed to 37 °C for 2 min (*Cold + RW*). All platelets were permeabilized with OG. Some OG-permeabilized platelets were further treated with 0.1% Triton X-100 after the temperature shifts to guarantee complete permeabilization and access of the pyrene-actin probe. The *bars* show the mean ± S.D. for five separate experiments.

We verified this idea by extracting OG-permeabilized cells with Triton X-100 after cooling, followed or not by rewarming. After Triton X-100 treatment, 199 ± 30 barbed end nucleation sites were detectable in chilled platelets, an increase of 3-fold over cells maintained at 37 °C. Chilling of OG-permeabilized platelets for ≥5 min at 4 °C followed by rewarming led to the production of 170 ± 10 barbed ends/cell, demonstrating that the permeabilized cells retain ~90% of their response to cold. Exposure of filament ends was restricted to barbed ends in OG-permeabilized platelets, since 2 μM cytochalasin B, an agent that binds to the barbed end and inhibits monomer assembly onto this end, abolished all detectable actin assembly from OG-permeabilized platelets (data not shown). In summary, cooling and rewarming of permeabilized platelets reports barbed end exposure and allows dissection of this process through the addition of inhibitory reagents normally unable to penetrate into platelets.

A ppI-binding Peptide Inhibits Actin Filament Barbed End Exposure in Response to Cold—The addition of a 10-mer peptide derived from the ppI-binding site of gelsolin to OG-permeabilized platelets diminished barbed actin filament end exposure when permeabilized platelets were chilled for 5 min. 2 μM peptide decreased detectable barbed ends by ~65%, and 20–30 μM completely inhibited barbed end exposure following chilling (Fig. 2*a*). Resting platelets have 44 ± 16 exposed actin filaments barbed ends. This result is consistent with previous studies showing that 25 μM of the 10-mer peptide inhibits all barbed end nucleation in permeabilized PAR-1-activated platelets and formyl-methionine-leucine-phenylalanine-activated neutrophils (9, 34). Incubation with 25 μM of the 10-mer peptide prevented the growth of protrusions from the surface of chilled permeabilized platelets (Fig. 2*b*). The addition of PtdIns-4,5-P_2 to OG-permeabilized, peptide-treated platelets rescued actin nucleation in a dose-dependent manner, whereas phosphatidylserine (*PS*) was without effect (Fig. 2*c*). These data show that ppIs are intimately involved in the actin assembly reaction that distorts the shape of the platelet in the cold. To determine whether the ppI content changes during the chilling process, platelets, loaded with ^{32}P to label the phospholipid pool, were incubated at ice bath temperatures for 5–40 min. Fig. 3 shows that cooling did not alter the content of D3- and D4-containing ppIs in platelet membranes at time points when actin assembly and shape change are maximal.

Formation of Barbed End Nucleation Sites is Temperature-dependent—To determine the temperature dependence of cold-induced actin assembly, platelets were incubated at decreasing temperatures for 5 min. As the temperature decreased, the barbed end number per platelet increased from 55 ± 9 at 37 °C to maximal values at or below 10 °C of 254 ± 21 barbed ends per cell. The platelet F-actin content increased maximally by ~25% at temperatures of ≤15 °C. Both barbed end exposure and F-actin content begin to increase when the temperature decreases to ≤20 °C. Tablin *et al.* (22) have shown that membrane phase transitions and platelet shape changes begin at this temperature. Platelets lose their responsiveness as their temperatures decrease and do not respond to TRAP at ≤5 °C (Fig. 4*a*).

GDPβS and Dominant Negative GTPases Do Not Inhibit the Cold-mediated Actin Filament Barbed End Exposure—When platelets are activated at 37 °C by ligation of the PAR-1 receptor, GTPases are upstream of ppI production (9, 10). As reported, GTPase antagonists, GDPβS or dominant negative GTPases, are potent inhibitors of PAR-1-mediated signaling to actin in platelets (9). Fig. 5 shows that actin assembly is not coupled to GTPases in chilled OG-permeabilized platelets. The nonhydrolyzable GDPβS and GTPγS analogs fail to affect the number of barbed ends exposed after chilling of OG-permeabilized platelets. In accordance with this finding, the dominant negative GTPases, 1.5 μM GST-N17Rac1 or 3 μM GST-N17Cdc42, do not affect the number of barbed filament ends produced in chilled OG-permeabilized platelets (Fig. 5). These data, combined with a lack of new ppI synthesis in the cold and the temperature dependence of barbed end exposure, support the notion that lipid rearrangements, uncoupled from receptors and GTPases, induce actin assembly and shape change in cooled platelets.

Barbed End Capping Proteins—Barbed end capping proteins such as gelsolin or adducin regulate platelet actin assembly. In the resting platelet, gelsolin is inactive, and most of it is not bound to actin and therefore extractable by detergents (35). Binding to actin by gelsolin is rapidly induced by the intracellular free calcium increase following PAR-1 ligation. A large fraction of the bound gelsolin subsequently dissociates from actin. Fig. 6*a* shows that gelsolin reversibly associates with the actin cytoskeleton fraction of chilled platelets. Gelsolin is ~80–90% detergent-extractable in resting platelets at 37 °C, but 20–30% becomes inextractable ≤5 min after chilling. In contrast, the small amount of gelsolin in the resting cytoskeleton (10%) dissociates from the cytoskeletal fraction of EGTA-AM-loaded and cooled platelets (Fig. 6*a*). As we previously reported, platelet F-actin content increased following cooling (4). The

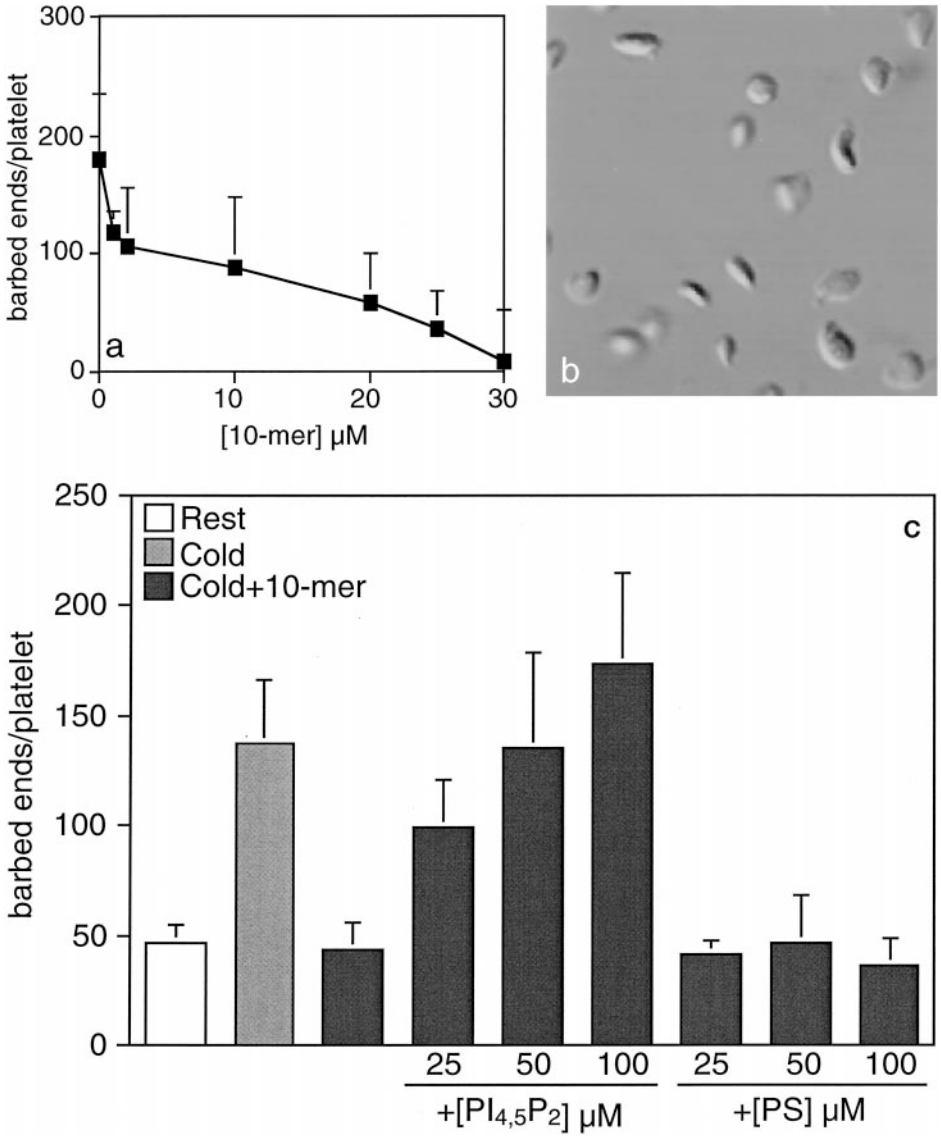

FIG. 2. **A peptide that binds and sequesters ppIs greatly diminishes the exposure of barbed end directed actin nucleation sites induced by cold.** *a*, effect of the gelsolin-derived ppI-binding peptide on the number of free barbed ends exposed in OG-permeabilized and chilled platelets. The peptide was added after OG-permeabilization and before chilling and rewarming of the platelets. *b*, chilling of OG-permeabilized platelets in the presence of 25 μM of the gelsolin-derived ppI-binding peptide prevents the bulk of the shape change induced by cooling. Peptide-treated platelets lack cellular protrusions although some cells still convert from discs into more spherical shapes. *c*, PtdIns-4,5-P_2 reverses the inhibition of nucleation induced by chilling. PtdIns-4.5-P4 or phosphatidylserine (*PS*) micelles were added to OG-permeabilized platelets treated with a 25 μM concentration of the gelsolin-derived ppI-binding peptide. Actin nucleation was recovered only in the presence of PtdIns-4,5-P_2. The *bars* show the mean ± S.D. for three separate experiments.

F-actin content increases from 40 to ~60% after chilling for 30 min, as determined by FITC-phalloidin binding by flow cytometry (data not shown) (4). The *inset* in Fig. 6*a* shows the gelsolin/F-actin ratio in cooled untreated platelets and in platelets preloaded with 40 μM EGTA-AM. The ratio increases from 1:300 in resting cells to 1:180 after 5 min of cooling and then decreases to 1:250 after 30 min of chilling. In contrast, the ratio decreased to 1:1000 within the first minute of cooling in platelets loaded with EGTA-AM. Direct evidence that gelsolin is involved in the actin response induced by chilling comes from experiments on platelets from gelsolin −/− mice. Fig. 6*b* shows that gelsolin −/− platelets undergo only small distortions from their discoid shape when cooled compared with wild-type mouse platelets. The most prominent shape change is the elongation of the discs into barbell shapes, although a few filopodia and blebs are observable. Wild-type mouse platelets lose their discoid shapes and protrude filopodia and blebs in similar fashion to human platelets when chilled. Gelsolin −/− platelets expose 50% less barbed ends upon chilling compared with gelsolin +/+ platelets. Fig. 6*c* reports that cold activation stimulates a ~3-fold increase of barbed end exposure in wild-type mouse platelets, whereas gelsolin −/− platelets have only a ~1.5-fold increase in barbed ends. Exposure of filament ends is restricted to the barbed ends in the Triton X-100 permeabilized platelets, since 2 μM cytochalasin B abolished all detectable pyrene actin assembly (data not shown). Murine platelets activated with 1 unit/ml thrombin for 1 min at 37 °C increased the number of actin nuclei by ~5-fold in wild-type and ~2.8-fold in the gelsolin null platelets.

Chilling also dissociates the barbed end capping protein adducin from the platelet actin cytoskeleton (Fig. 7). In resting platelets, ~70–80% of the total adducin is bound to the cytoskeletal fraction. Adducin begins to dissociate from the platelet actin cytoskeleton 2 min after chilling, and the dissociation becomes maximal after 30 min (Fig. 7). The *inset* in Fig. 7 shows the adducin/F-actin ratio in the cytoskeleton of cold-activated platelets. The amount of adducin bound to the cytoskeletal fraction decreases during the cold activation 1:100 in resting cells to 1:333 after 30 min. The distribution of CapZ, a barbed end capping protein that terminates actin filament assembly by capping the ends of elongating filaments (36–38), did not change following cooling of platelets (data not shown).

Role of the Arp2/3 Complex in the Platelet Actin Assembly Induced by Chilling—To determine whether the Arp2/3 complex participates in cold-induced actin assembly of OG-permeabilized platelets, we used constructs derived from N-WASp that inhibit Arp2/3 complex-mediated actin nucleation. The C-terminal CA domain of N-WASp (amino acids 450–505) binds to the Arp2/3 complex, inhibiting its function. In contrast, N-WASp VCA domain (amino acids 392–505) binds to

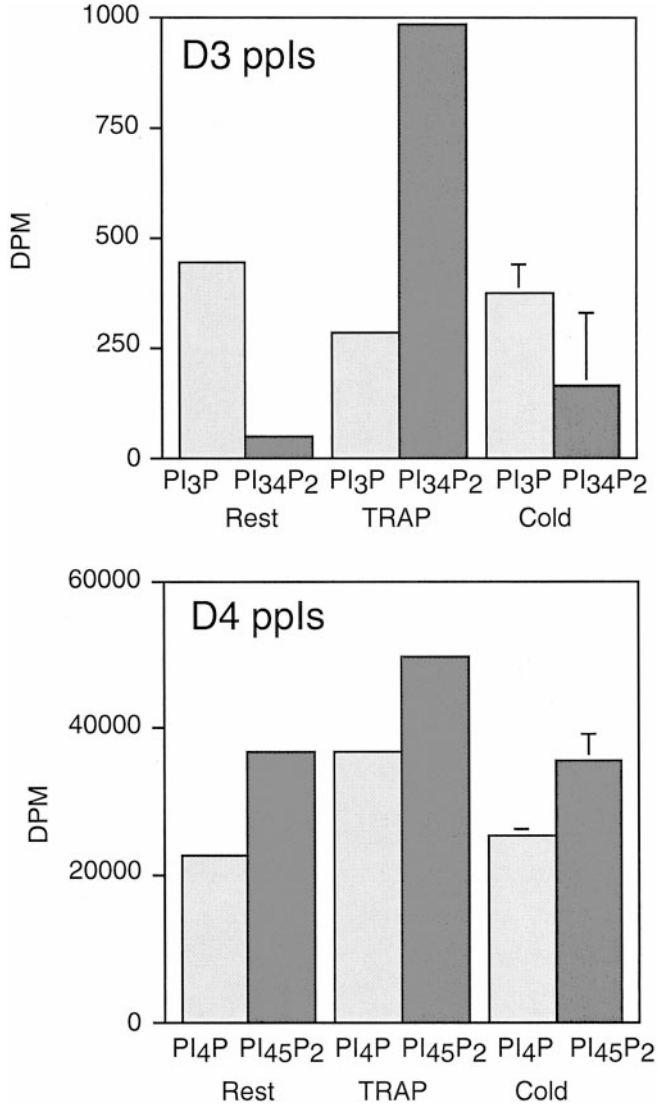

FIG. 3. **Chilling of platelets to 4 °C does not result in the synthesis or degradation of membrane ppIs.** Platelet ppIs, labeled to equilibrium with ^{32}P, were isolated from resting and chilled platelets. The relative distribution of each ppI type was quantified by HPLC analysis. Profiles are shown of phosphatidylinositol 3-trisphosphate (PI_3P) and phosphatidylinositol 3,4-bisphosphate ($PI_{34}P_2$) (*top*) and of phosphatidylinositol 4-phosphate (PI_4P) and PtdIns-4,5-P_2 ($PI_{45}P_2$) (*bottom*) in platelets incubated at ice bath temperatures for 5–40 min.

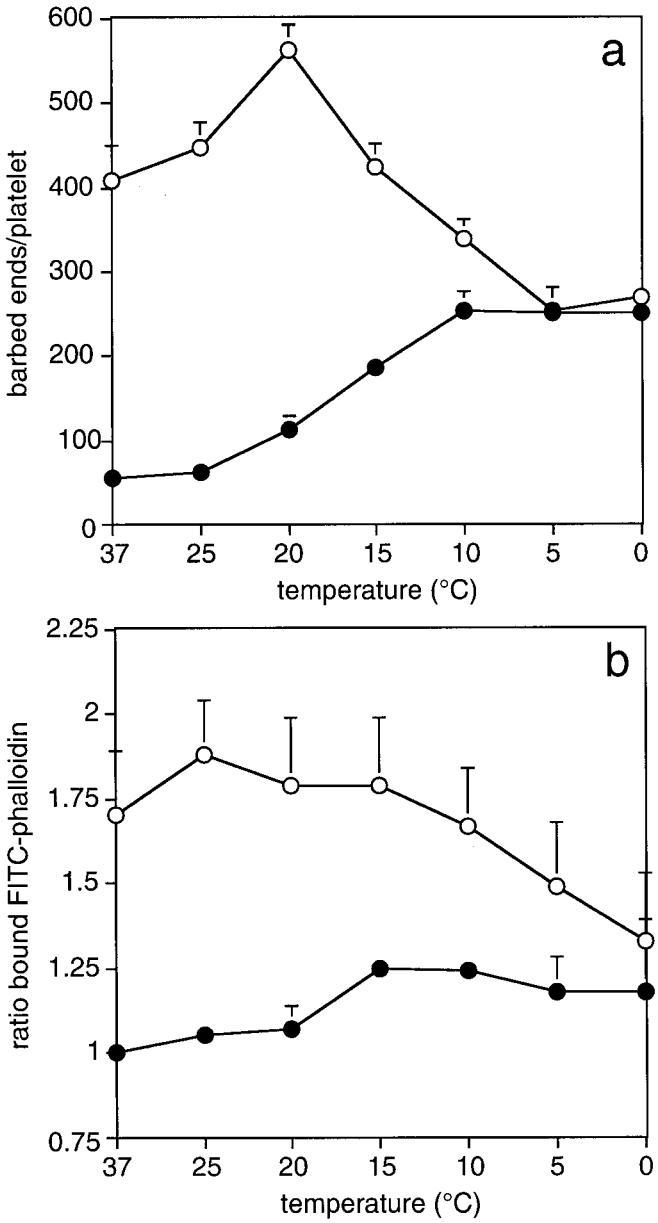

FIG. 4. **Temperature dependence of the formation of barbed end nucleation sites and actin assembly.** Platelets were incubated at various temperatures (37, 25, 20, 15, 10, 5, or 0 °C) for 5 min. *a*, barbed ends were counted before (*closed circles*) or after the addition of 25 μM TRAP for 60 s (*open circles*). *b*, F-actin content was measured before (*closed circles*) or after the addition of 25 μM TRAP for 60 s (*open circles*). The values of both experiments are the means ± S.D. of six individual points.

actin monomers and the Arp2/3 complex and leads to an enhancement of actin nucleation (20). GST-CA added to the OG-permeabilized platelets before chilling inhibits the barbed end number induced by chilling in a concentration-dependent manner (Fig. 8). The addition of >0.1 μM of GST-CA to the OG-permeabilized platelets diminished the number of barbed ends measurable after chilling by ~40% (Fig. 8), indicating that Arp2/3 activation contributes about half the nuclei used in the actin assembly reaction of chilled platelets.

DISCUSSION

Our results show that actin assembly observed during cold activation of platelets results from membrane lipid rearrangements without activation of GTPases and synthesis of ppIs. The mechanics of cold activation involve known regulatory processes of actin assembly. First is the activation of gelsolin to sever actin filaments through increased intracellular calcium (23, 35). Cooling of platelets leads to a slow rise in free cytosolic calcium to levels of 200–300 nM (4, 39), which is not surprising, because cold decreases the activity of calcium pumps that function to extrude calcium (40). In chilled platelets, gelsolin, the major actin filament-severing protein of platelets, transiently associates with the actin cytoskeleton and becomes maximally bound after 5 min. Translocation into the cytoskeleton is prevented if platelets are loaded with EGTA. We previously demonstrated barbed end exposure to be inhibited by ~50% in Quin2-loaded platelets, consistent with the loss of calcium-activated gelsolin severing activity (4). Second is the exposure of actin filament barbed ends that induce new actin assembly by ppIs (9). ppIs are known to be intimately involved in the barbed end-based nucleation and actin assembly of PAR-1-activated platelets (9). Unlike PAR-1-mediated activation, barbed end exposure/nucleation is uncoupled in the cold from GTPases and ppI synthesis. The addition of GDPβS or the negative dominant Rho family GTPases N17Cdc42 or N17Rac

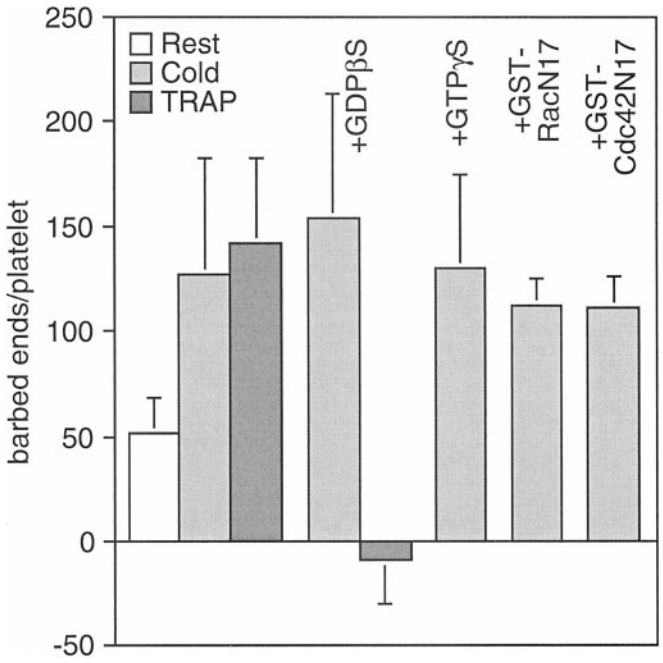

FIG. 5. **The production of barbed end directed nucleation sites is uncoupled from GTPases.** Effect of treating OG-permeabilized platelets with the guanine nucleotide analogs GDPβS or GTPγS on the number of free actin filament barbed end nucleation sites in resting or chilled platelets for 5 min (*Cold*). OG-permeabilized platelets were also treated with 25 μM TRAP for 1 min at 37 °C in the absence and presence of GDPβS. GDPβS has been shown previously to inhibit barbed end exposure mediated by TRAP. Negative dominant GTPases do not block the exposure of actin filament nucleation sites induced by cooling. Effects of bacterially expressed GST-N17Rac1 (1.5 μM) or GST-N17Cdc42 (3 μM) on the number of barbed filament ends in OG-permeabilized chilled platelets. Values are mean ± S.D. for five individual experiments.

did not effect barbed end exposure in permeabilized and chilled platelets.

To investigate whether the cold-induced actin assembly observed in platelets involves ppI-mediated uncapping of filaments, we applied a permeabilization scheme used to define the mechanisms of the PAR-1-mediated actin assembly in platelets and formyl-methionine-leucine-phenylalanine-induced actin assembly in polymorphonuclear leukocytes (9, 34). Platelets, briefly permeabilized with OG, were chilled to 4 °C, and shape change and actin assembly were monitored. After chilling, blebs and protrusions developed on the surfaces of OG-permeabilized platelets in similar fashion to those extruded by chilled intact platelets (43). These findings demonstrate that OG-treated platelets retain their response to cold in terms of actin-driven shape change. Cold induced the formation of ~200 new barbed filament ends per platelet within 5 min, consistent with our previous study showing barbed end exposure to increase within minutes when platelets were shifted to ice bath temperature (4). This number of barbed ends represents ~40% of the total barbed end number exposed following PAR-1 activation (9). Treatment of OG-permeabilized platelets with a peptide that binds and sequesters ppIs prevents cold-induced protrusive activity and blocks all barbed end exposure. The inhibitory effect of the ppI binding peptide on actin assembly was rescued by the addition of PtdIns-4,5-P_2 micelles to the OG-permeabilized and chilled platelets. This demonstrates that ppIs are involved in the reactions that lead to barbed end exposure/nucleation in the cold.

Since net ppI synthesis or degradation was not observed following chilling, we propose that a structural change of ppIs in the membrane induces the exposure of actin filament barbed ends and the induction of actin assembly. The temperature dependence of barbed end exposure correlates with that of the membrane phase transition and would change lipid packing, causing ppI clustering (22). Aggregation of ppIs would potentiate the activity of the phosphoinositol-lipid head groups in the platelet plasma membrane as has been shown for ppIs in mixed lipid vesicles *in vitro* (41). The aggregation process would also be predicted to occur independently of the activity of GTPases, as observed.

Targets of ppIs—Targets of these phospholipid clusters include barbed end capping proteins and the Arp2/3 complex. The uncapping of actin filament barbed ends was the first pathway defined to be involved in ppI-induced actin assembly, and evidence has been provided by us that barbed end capping proteins are released from actin filaments during cell activation by the addition of ppIs to permeabilized platelets (36). Our data are consistent with the idea that 50–60% of the barbed end-based nucleation activity in chilled platelets derives from actin filaments severed by gelsolin and subsequently uncapped. The small amount of gelsolin associated with the resting cytoskeleton dissociates when EGTA-AM-loaded platelets are chilled for 5 min, indicating that signals (ppIs) that dissociate gelsolin from actin remain intact in these cells. A similar dissociation from the cytoskeletal fraction was observed after 30 min in untreated cooled platelets. In addition gelsolin-deficient platelets were found to be less responsive to chilling and to produce only 50% of barbed end nucleation sites of normal platelets.

Adducin is a second platelet protein that may contribute to the actin nucleation induced by ppIs. Adducin was first identified as a barbed end capping protein in the membrane cytoskeleton of red blood cells (42, 43). Adducin possesses a myristoylated alanine-rich protein kinase C substrate-related domain that is required for its actin filament barbed end capping activity (44). This 25-amino acid basic domain is phosphorylated at multiple serines by protein kinase C and also binds to calmodulin or PtdIns-4,5-P_2 to regulate its interaction with actin (45, 46). In the resting platelet, 70–80% of the total adducin is associated with the actin cytoskeleton. Chilling dissociates adducin from the cytoskeleton. Adducin's dissociation could be due to the calcium activation of calmodulin in chilled platelets or, since the gelsolin-derived ppI-binding peptide completely inhibits cold-induced barbed end exposure, by phospholipid binding within this myristoylated alanine-rich protein kinase C substrate domain. It is not clear yet which mechanism is involved, but dissociation of adducin from actin filaments is expected to contribute to barbed end exposure.

A more recently discovered mechanism leading to cytoplasmic actin assembly is the *de novo* actin nucleation by the Arp2/3 complex (19, 20, 47–51). We investigated whether the Arp2/3 complex participates in cold-induced actin assembly by adding a negative dominant inhibitor of its function (GST-CA) to the permeabilized platelets. GST-CA inhibits the barbed end production induced through chilling by ~40% when added to OG-permeabilized platelets prior to chilling. The Arp2/3 complex nucleates actin downstream of WASp family proteins (WASp, N-WASp, Scar/WAVE), which require GTPases and ppIs to become active (20, 52, 53). PtdIns-4,5-P_2 and the small GTPase Cdc42 co-activate N-WASp (20). N-WASp can be activated by PtdIns-4,5-P_2 micelles alone, whereas GTPCdc42 is a poor activator of N-WASp in the absence of PtdIns-4,5-P_2 (53).

Temperature Dependence of the Cold-induced Response—It is well established that platelets begin to change shape at temperatures of <25 °C and that the number of activated platelets increases with decreasing temperatures until 5 °C (22). We investigated the relation of temperature to the barbed end nucleation activity in platelets and found that free barbed end

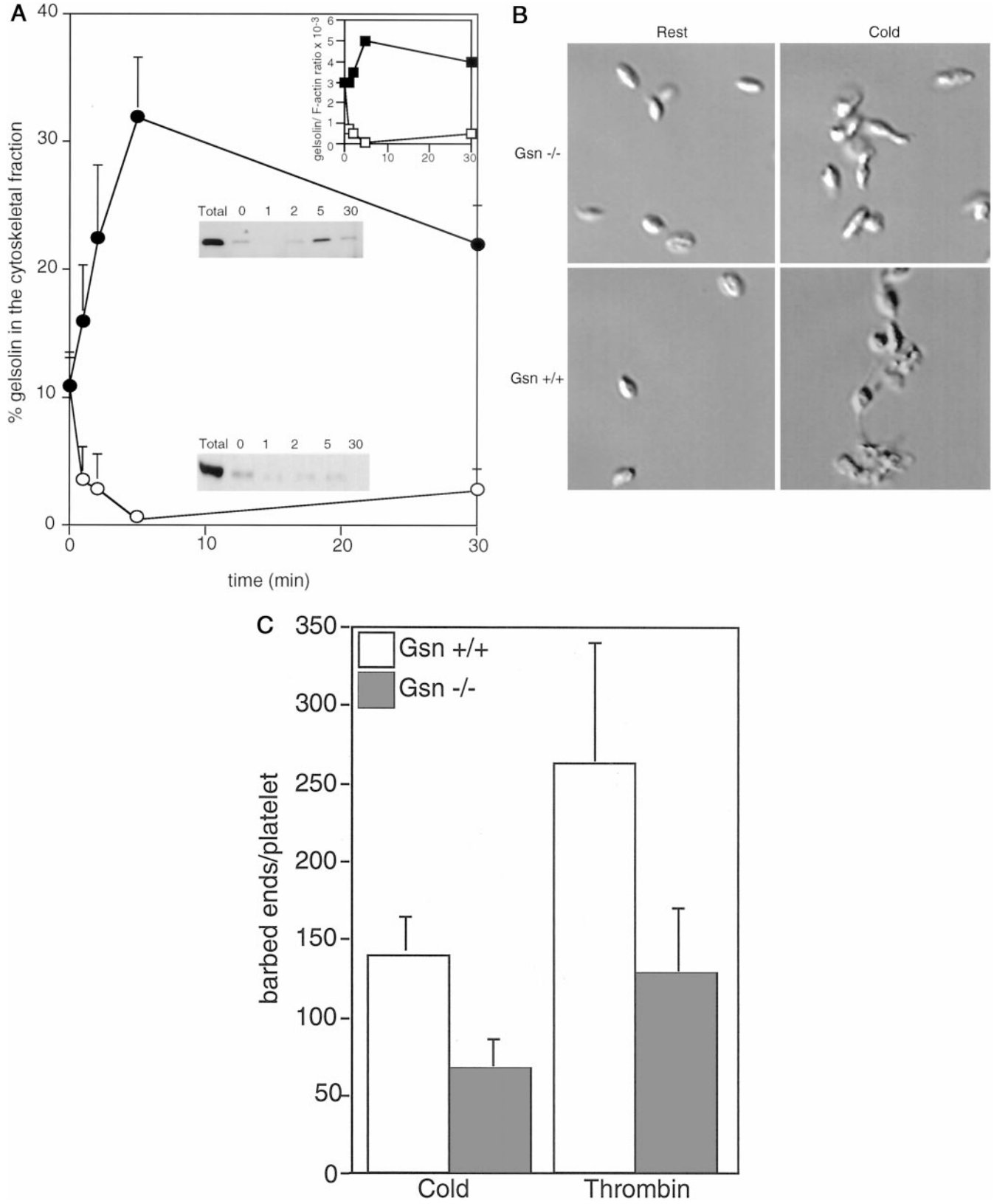

FIG. 6. **Role of gelsolin in barbed end exposure mediated by cooling.** *A*, interaction of gelsolin with the actin cytoskeleton of untreated chilled platelets (*closed circles*) or platelets first incubated with 40 μM EGTA-AM for 30 min (*open circles*). Soluble gelsolin was separated from cytoskeletal bound gelsolin in Triton X-100 platelet lysates by centrifugation at 450,000 $\times$ *g* for 30 min. Gelsolin was detected by immunoblotting. The graphs quantify the movement of gelsolin into the platelet cytoskeleton. The values are the means $\pm$ S.D. for three individual experiments. The *inset* shows the gelsolin/F-actin ratio in the cytoskeleton of chilled platelets (*closed squares*) and platelets preloaded with EGTA-AM and then chilled (*open squares*). *B*, gelsolin $-/-$ platelets have a diminished shape change response to chilling compared with wild-type mouse platelets. The *panel* compares the morphology of resting (*Rest*) and chilled (*Cold*) platelets of wild-type (Gsn +/+) and gelsolin $-/-$ mice. *C*, gelsolin $-/-$ platelets expose fewer barbed end nucleation sites when chilled compared with normal mouse platelets. Actin nucleation sites when quantified in Triton X-100 permeabilized gelsolin +/+ and gelsolin $-/-$ platelets chilled for 5 min or stimulated with 1 unit/ml thrombin for 1 min. The resting barbed end numbers were 65 $\pm$ 4 in wild-type platelets and 83 $\pm$ 16 in gelsolin $-/-$ platelets.

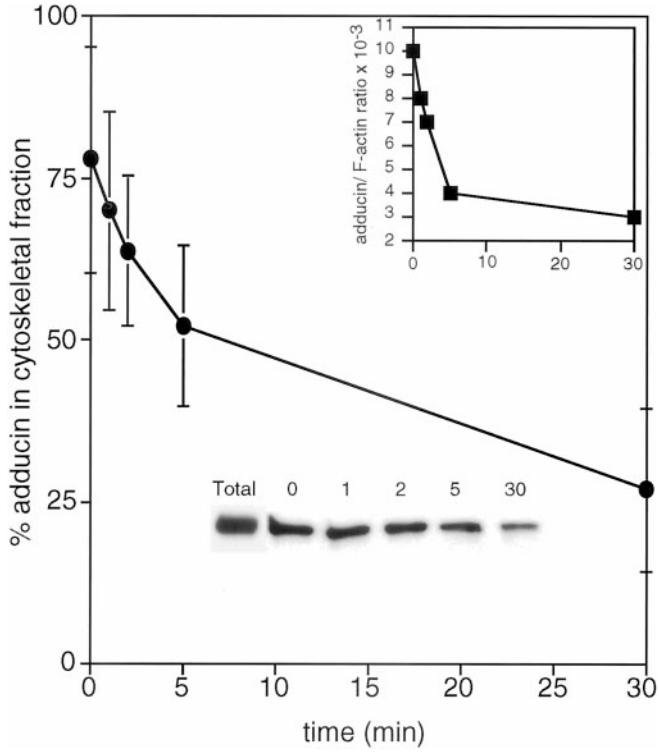

FIG. 7. **Chilling dissociates adducin from the platelet cytoskeleton.** Time course of adducin release from the cytoskeleton as detected by immunoblotting of soluble and insoluble fractions of lysates of chilled platelets (*circles*). The *inset* shows the adducin/F-actin ratio during cooling (*squares*). The data are the mean ± S.D. for three experiments.

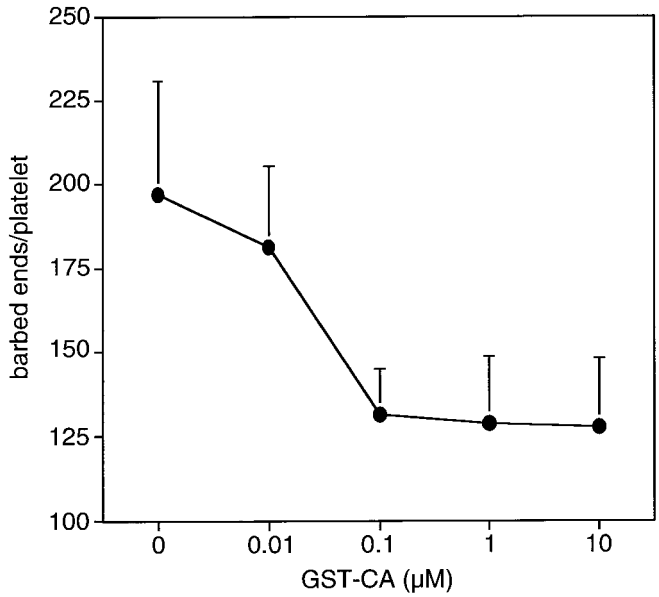

FIG. 8. **Role of the Arp2/3 complex in the formation of barbed end nucleation sites induced by chilling to 4°C.** Shown is dose response for the inhibition of barbed end nuclei by the dominant negative N-WASp C terminus (GST-CA) construct in response to the activation of OG-permeabilized platelets through chilling. The addition of saturating concentrations of GST-CA reduced by ~40% the production/exposure of barbed end-directed nucleation sites in OG-permeabilized chilled platelets. The resting barbed end numbers were 57 ± 19. The values are the means ± S.D. for three individual experiments.

nucleation begins at temperatures of <25 °C, as has been reported for the membrane phase transitions that change the packing of membrane lipids (22). As platelets are activated by cold, they lose their ability to respond to receptor-mediated stimuli. Below 5 °C, platelets lack responsiveness to TRAP. Although we expected barbed end nucleation in platelets induced by TRAP to be maximal at 37 °C, higher barbed end nucleation and actin assembly were found in platelets activated at 20–25 °C. These results imply that at 20–25 °C nucleation activity derives from the combined effects of temperature-induced nucleation and the normal receptor-coupled signaling events. It also suggests that the exquisite sensitivity of platelets to temperature may lead to a coupling of membrane dynamics and signaling events mediating a maximal physiological response at temperatures below 37 °C, such as those that exist in dermis and at wound sites.

Our data show that platelet actin filament assembly induced by cooling requires membrane ppIs to mediate the uncapping of actin filaments by gelsolin and adducin and *de novo* actin nucleation by the Arp2/3 complex. However, the signaling pathways are uncoupled from receptors and small GTPases. The data lead to a better understanding of how cooling leads to platelet shape changes and actin assembly and shows their sensitivity to temperature changes. This knowledge may contribute to a better storage of platelets.

Acknowledgments—We thank Laurice Salib and Natasha Isaac for excellent technical assistance and Karen Vengerow for stylistic revision to the manuscript.

REFERENCES

1. White, J., and Krivit, W. (1967) *Blood* **30,** 625–635
2. White, J., and Krumwiede, M. (1973) *Blood* **41,** 823–832
3. White, J. (1982) *Am. J. Pathol.* **108,** 184
4. Winokur, R., and Hartwig, J. (1995) *Blood* **85,** 1796–1804
5. Zucker, M., and Borrelli, J. (1954) *Blood* **28,** 524–534
6. Chernoff, A., and Snyder, E. (1992) *Transfusion* **32,** 386–390
7. Moroff, G., Holme, S., George, V., and Heaton, W. (1994) *Transfusion* **34,** 317–321
8. White, J. (1968) *Am. J. Pathol.* **53,** 281–291
9. Hartwig, J., Bokoch, G., Carpenter, C., Janmey, P., Taylor, L., Toker, A., and Stossel, T. (1995) *Cell* **82,** 643–653
10. Tolias, K., Hartwig, J., Ishihara, H., Shibisaki, Y., Erickson, J., Cantley, L., and Carpenter, C. (2000) *Curr. Biol.* **10,** 153–156
11. Derry, J., Ochs, H., and Francke, U. (1994) *Cell* **78,** 635–644
12. Kolluri, R., Tolias, K., Carpenter, C., Rosen, F., and Kirchhausen, T. (1996) *Proc. Natl. Acad. Sci. U. S. A.* **93,** 5615–5618
13. Symons, M., Derry, J., Karlak, B., Jiang, S., Lemahieu, V., McCormick, F., Francke, U., and Abo, A. (1996) *Cell* **84,** 723–734
14. Aspenstrom, P., Lindberg, U., and Hall, A. (1996) *Curr. Biol.* **6,** 70–75
15. Miki, H., Miura, K., and Takenawa, T. (1996) *EMBO J.* **15,** 5326–5335
16. Gross, B., Wilde, J., Quek, L., Cahpel, H., Nelson, D., and Watson, S. (2000) *Blood* **94,** 4166–4176
17. Machesky, L., and Gould, K. (1999) *Curr. Opin. Cell Biol.* **11,** 117–121
18. Machesky, L., and Insall, R. (1998) *Curr. Biol.* **8,** 1347–1354
19. Machesky, L., Mullins, R., Higgs, H., Kaiser, D., Blanchoin, L., May, R., Hall, M., and Pollard, T. (1999) *Proc. Natl. Acad. Sci. U. S. A.* **96,** 3739–3744
20. Rohatgi, R., Ma, L., Miki, H., Lopez, M., Kirchhausen, T., Takenawa, T., and Kirschner, M. (1999) *Cell* **97,** 221–231
21. Janmey, P., and Stossel, T. (1989) *J. Biol. Chem.* **264,** 4825–4831
22. Tablin, F., Oliver, A., Walker, N., Crowe, L., and Crowe, J. (1996) *J. Cell. Physiol.* **168,** 305–313
23. Hartwig, J. (1992) *J. Cell Biol.* **118,** 1421–1442
24. Janmey, P., Lamb, J., Allen, P., and Matsudaira, P. (1992) *J. Biol. Chem.* **267,** 11818–11823
25. Chaponnier, C., Yin, H. L., and Stossel, T. P. (1987) *J. Exp. Med.* **165,** 97–106
26. Hartwig, J., and DeSisto, M. (1991) *J. Cell Biol.* **112,** 407–425
27. Witke, W., Sharpe, A., Hartwig, J., Azuma, T., Stossel, T., and Kwiatkowski, D. (1995) *Cell* **81,** 41–51
28. Falet, H., Barkalow, K. L., Pivniouk, V. I., Barnes, M. J., Geha, R. S., and Hartwig, J. H. (2000) *Blood* **96,** 3786–3792
29. Hartwig, J. (1992) *The Cytoskeleton: A Practical Approach*, (Carraway, K. L., and Carraway, C.-A. C., eds) pp. 23–45, Oxford University Press, Oxford, UK
30. Hartwig, J., Kung, S., Kovacsovics, T., Janmey, P., Cantley, L., Stossel, T., and Toker, A. (1996) *J. Biol. Chem.* **271,** 32986–32993
31. Toker, A. (1998) *Curr. Opin. Cell Biol.* **10,** 254–261
32. Pollard, T. (1986) *J. Cell Biol.* **103,** 2747–2754
33. Laemmli, U. (1970) *Nature* **227,** 680–685
34. Glogauer, M., Hartwig, J., and Stossel, T. (2000) *J. Cell Biol.* **150,** 785–796
35. Lind, S. E., Janmey, P. A., Chaponnier, C., Herbert, T.-J., and Stossel, T. P. (1987) *J. Cell Biol.* **105,** 833–842
36. Barkalow, K., Witke, W., Kwiatkowski, D., and Hartwig, J. (1996) *J. Cell Biol.* **134,** 389–399
37. Eddy, R., Han, J., and Condeelis, J. (1997) *J. Cell Biol.* **139,** 1243–1253
38. Nachmias, V., Golla, R., Casella, J., and Barron-Casella, E. (1996) *FEBS Lett.* **378,** 258–262
39. Bennett, W. F., and Lynch, G. (1980) *J. Cell Biol.* **86,** 280–285
40. Vostal, J. G., Jackson, W. L., and Shulman, N. R. (1991) *J. Biol. Chem.* **266,**

16911–16916
41. Janmey, P. (1994) *Annu. Rev. Physiol.* **56,** 169–191
42. Kuhlman, P., Hughes, C., Bennett, V., and Fowler, V. (1996) *J. Biol. Chem.* **271,** 7986–7991
43. Matsuoka, Y., Li, X., and Bennett, V. (2000) *Cell. Motil. Life Sci.* **57,** 884–895
44. Li, X., Matsuoka, Y., and Bennett, V. (1998) *J. Biol. Chem.* **273,** 19329–19338
45. Aderem, A. (1992) *Cell* **71,** 713–716
46. Hartwig, J., Thelen, M., Rosen, A., Janmey, P., Nairn, A., and Aderem, A. (1992) *Nature* **356,** 618–622
47. Welch, M., Rosenblatt, J., Skoble, J., Portnoy, D., and Mitchison, T. (1998) *Science* **281,** 105–108
48. Mullins, R., and Pollard, T. (1999) *Curr. Biol.* **9,** 405–415
49. Ma, L., Rohatgi, R., and Kirschner, M. (1998) *Proc. Natl. Acad. Sci. U. S. A.* **95,** 15362–15367
50. Svitkina, T., and Borisy, G. (1999) *J. Cell Biol.* **145,** 1009–1026
51. Loisel, T., Boujemaa, R., Pataloni, D., and Carlier, M.-F. (1999) *Nature* **401,** 613–616
52. Rohatgi, R., Ho, H. H., and Kirschner, M. W. (2000) *J. Cell Biol.* **150,** 1299–1309
53. Higgs, H. N., and Pollard, T. D. (2000) *J. Cell Biol.* **150,** 1311–1320